

Measurement of the Polarized Structure Function $\sigma_{LT'}$ for Pion Electroproduction in the Roper Resonance Region

K. Joo,¹ L.C. Smith,² I.G. Aznauryan,³ V.D. Burkert,⁴ H. Egiyan,^{38,4,*} R. Minehart,² G. Adams,³²
P. Ambrozewicz,¹³ E. Anciant,⁹ M. Anghinolfi,¹⁹ B. Asavapibhop,²⁵ G. Asryan,³ G. Audit,⁹ T. Auger,⁹
H. Avakian,^{18,4} H. Bagdasaryan,³⁰ N. Baillie,³⁸ J.P. Ball,⁵ N.A. Baltzell,³⁵ S. Barrow,¹⁴ V. Batourine,²³
M. Battaglieri,¹⁹ K. Beard,²² I. Bedlinskiy,²¹ M. Bektasoglu,^{29,†} M. Bellis,⁷ N. Benmouna,¹⁵ B.L. Berman,¹⁵
N. Bianchi,¹⁸ A.S. Biselli,^{32,7} B.E. Bonner,³³ S. Bouchigny,^{4,20} S. Boiarinov,^{21,4} R. Bradford,⁷ D. Branford,¹²
W.J. Briscoe,¹⁵ W.K. Brooks,⁴ S. Bueltmann,³⁰ C. Butuceanu,³⁸ J.R. Calarco,²⁷ S.L. Careccia,³⁰ D.S. Carman,²⁹
B. Carnahan,⁸ C. Cetina,¹⁵ S. Chen,¹⁴ P.L. Cole,^{4,17} A. Coleman,^{38,‡} P. Coltharp,¹⁴ D. Cords,⁴ P. Corvisiero,¹⁹
D. Crabb,² J.P. Cummings,³² E. De Sanctis,¹⁸ R. DeVita,¹⁹ P.V. Degtyarenko,⁴ L. Dennis,¹⁴ A. Deur,⁴
K.V. Dharmawardane,³⁰ K.S. Dhuga,¹⁵ C. Djalali,³⁵ G.E. Dodge,³⁰ J. Donnelly,¹⁶ D. Doughty,^{10,4}
P. Dragovitsch,¹⁴ M. Dugger,⁵ S. Dytman,³¹ O.P. Dzyubak,³⁵ K.S. Egiyan,³ L. Elouadrhiri,^{10,4} A. Empl,³²
P. Eugenio,¹⁴ L. Farhi,⁹ R. Fatemi,² G. Fedotov,²⁶ G. Feldman,¹⁵ R.J. Feuerbach,⁷ T.A. Forest,³⁰ V. Frolov,³²
H. Funsten,³⁸ S.J. Gaff,¹¹ M. Garçon,⁹ G. Gavalian,³⁰ G.P. Gilfoyle,³⁴ K.L. Giovanetti,²² P. Girard,³⁵ F.X. Girod,⁹
J.T. Goetz,⁶ R.W. Gothe,³⁵ K.A. Griffioen,³⁸ M. Guidal,²⁰ M. Guillo,³⁵ N. Guler,³⁰ L. Guo,⁴ V. Gyurjyan,⁴
R.S. Hakobyan,⁸ J. Hardie,^{10,4} D. Heddle,^{10,4} F.W. Hersman,²⁷ K. Hicks,²⁹ I. Hleiqawi,²⁹ M. Holtrop,²⁷
J. Hu,³² C.E. Hyde-Wright,³⁰ Y. Ilieva,¹⁵ D.G. Ireland,¹⁶ B.S. Ishkhanov,²⁶ M.M. Ito,⁴ D. Jenkins,³⁷ H.S. Jo,²⁰
H.G. Juengst,¹⁵ J.H. Kelley,¹¹ J.D. Kellie,¹⁶ M. Khandaker,²⁸ K.Y. Kim,³¹ K. Kim,²³ W. Kim,²³ A. Klein,³⁰
F.J. Klein,^{4,8} A.V. Klimenko,³⁰ M. Klusman,³² M. Kossov,²¹ L.H. Kramer,^{13,4} V. Kubarovsky,³² J. Kuhn,⁷
S.E. Kuhn,³⁰ J. Lachniet,⁷ J.M. Laget,^{4,9} J. Langheinrich,³⁵ D. Lawrence,²⁵ T. Lee,²⁷ K. Livingston,¹⁶
K. Lukashin,^{4,§} J.J. Manak,⁴ C. Marchand,⁹ L.C. Maximon,¹⁵ S. McAleer,¹⁴ B. McKinnon,¹⁶ J.W.C. McNabb,⁷
B.A. Mecking,⁴ M.D. Mestayer,⁴ C.A. Meyer,⁷ K. Mikhailov,²¹ M. Mirazita,¹⁸ R. Miskimen,²⁵ V. Mokeev,^{26,4}
S.A. Morrow,^{9,20} V. Muccifora,¹⁸ J. Mueller,³¹ G.S. Mutchler,³³ P. Nadel-Turonski,¹⁵ J. Napolitano,³²
R. Nasseripour,^{13,¶} S.O. Nelson,¹¹ S. Niccolai,²⁰ G. Niculescu,^{29,22} I. Niculescu,^{15,22} B.B. Niczyporuk,⁴
R.A. Niyazov,⁴ M. Nozar,⁴ G.V. O'Rielly,¹⁵ M. Osipenko,^{19,26} A.I. Ostrovidov,¹⁴ K. Park,²³ E. Pasyuk,⁵
G. Peterson,²⁵ S.A. Philips,¹⁵ J. Pierce,² N. Pivnyuk,²¹ D. Pocanic,² O. Pogorelko,²¹ E. Polli,¹⁸ S. Pozdniakov,²¹
B.M. Preedon,³⁵ J.W. Price,⁶ Y. Prok,^{4,**} D. Protopopescu,¹⁶ L.M. Qin,³⁰ B.A. Raue,^{13,4} G. Riccardi,¹⁴
G. Ricco,¹⁹ M. Ripani,¹⁹ B.G. Ritchie,⁵ F. Ronchetti,¹⁸ G. Rosner,¹⁶ P. Rossi,¹⁸ D. Rowntree,²⁴ P.D. Rubin,³⁴
F. Sabatié,⁹ K. Sabourov,¹¹ C. Salgado,²⁸ J.P. Santoro,^{37,4} V. Sapunenko,^{19,4} R.A. Schumacher,⁷ V.S. Serov,²¹
A. Shafi,¹⁵ Y.G. Sharabian,^{3,4} J. Shaw,²⁵ S. Simionatto,¹⁵ A.V. Skabelin,²⁴ E.S. Smith,⁴ D.I. Sober,⁸ M. Spraker,¹¹
A. Stavinsky,²¹ S.S. Stepanyan,²³ S. Stepanyan,^{4,3} B.E. Stokes,¹⁴ P. Stoler,³² I.I. Strakovsky,¹⁵ S. Strauch,¹⁵
M. Taiuti,¹⁹ S. Taylor,³³ D.J. Tedeschi,³⁵ U. Thoma,^{4,††} R. Thompson,³¹ A. Tkabladze,²⁹ C. Tur,³⁵
M. Ungaro,¹ M.F. Vineyard,^{36,34} A.V. Vlassov,²¹ K. Wang,² L.B. Weinstein,³⁰ H. Weller,¹¹ D.P. Weygand,⁴
M. Williams,⁷ E. Wolin,⁴ M.H. Wood,^{35,‡‡} A. Yegneswaran,⁴ J. Yun,³⁰ L. Zana,²⁷ and J. Zhang³⁰

(The CLAS Collaboration)

¹ University of Connecticut, Storrs, Connecticut 06269

² University of Virginia, Charlottesville, Virginia 22901

³ Yerevan Physics Institute, 375036 Yerevan, Armenia

⁴ Thomas Jefferson National Accelerator Facility, Newport News, Virginia 23606

⁵ Arizona State University, Tempe, Arizona 85287-1504

⁶ University of California at Los Angeles, Los Angeles, California 90095-1547

⁷ Carnegie Mellon University, Pittsburgh, Pennsylvania 15213

⁸ Catholic University of America, Washington, D.C. 20064

⁹ CEA-Saclay, Service de Physique Nucléaire, F91191 Gif-sur-Yvette, France

¹⁰ Christopher Newport University, Newport News, Virginia 23606

¹¹ Duke University, Durham, North Carolina 27708-0305

¹² Edinburgh University, Edinburgh EH9 3JZ, United Kingdom

¹³ Florida International University, Miami, Florida 33199

¹⁴ Florida State University, Tallahassee, Florida 32306

¹⁵ The George Washington University, Washington, DC 20052

¹⁶ University of Glasgow, Glasgow G12 8QQ, United Kingdom

¹⁷ Idaho State University, Pocatello, Idaho 83209

¹⁸ INFN, Laboratori Nazionali di Frascati, Frascati, Italy

¹⁹ INFN, Sezione di Genova, 16146 Genova, Italy

²⁰ Institut de Physique Nucleaire ORSAY, Orsay, France

- ²¹*Institute of Theoretical and Experimental Physics, Moscow, 117259, Russia*
²²*James Madison University, Harrisonburg, Virginia 22807*
²³*Kyungpook National University, Daegu 702-701, South Korea*
²⁴*Massachusetts Institute of Technology, Cambridge, Massachusetts 02139-4307*
²⁵*University of Massachusetts, Amherst, Massachusetts 01003*
²⁶*Moscow State University, Skobeltsyn Nuclear Physics Institute, 119899 Moscow, Russia*
²⁷*University of New Hampshire, Durham, New Hampshire 03824-3568*
²⁸*Norfolk State University, Norfolk, Virginia 23504*
²⁹*Ohio University, Athens, Ohio 45701*
³⁰*Old Dominion University, Norfolk, Virginia 23529*
³¹*University of Pittsburgh, Pittsburgh, Pennsylvania 15260*
³²*Rensselaer Polytechnic Institute, Troy, New York 12180-3590*
³³*Rice University, Houston, Texas 77005-1892*
³⁴*University of Richmond, Richmond, Virginia 23173*
³⁵*University of South Carolina, Columbia, South Carolina 29208*
³⁶*Union College, Schenectady, NY 12308*
³⁷*Virginia Polytechnic Institute and State University, Blacksburg, Virginia 24061-0435*
³⁸*College of William and Mary, Williamsburg, Virginia 23187-8795*

The polarized longitudinal-transverse structure function $\sigma_{LT'}$ measures the interference between real and imaginary amplitudes in pion electroproduction and can be used to probe the coupling between resonant and non-resonant processes. We report new measurements of $\sigma_{LT'}$ in the $N(1440)_{\frac{1}{2}}^{+}$ (Roper) resonance region at $Q^2 = 0.40$ and 0.65 GeV² for both the $\pi^0 p$ and $\pi^+ n$ channels. The experiment was performed at Jefferson Lab with the CEBAF Large Acceptance Spectrometer (CLAS) using longitudinally polarized electrons at a beam energy of 1.515 GeV. Complete angular distributions were obtained and are compared to recent phenomenological models. The $\sigma_{LT'}(\pi^+ n)$ channel shows a large sensitivity to the Roper resonance multipoles M_{1-} and S_{1-} and provides new constraints on models of resonance formation.

PACS numbers: PACS : 13.60.Le, 12.40.Nn, 13.40.Gp

The structure of the $J^P = 1/2^+$ $N(1440)$ resonance continues to be a mystery more than 40 years after its discovery by Roper [1] in the P_{11} πN channel. Attention has largely centered on the inability of the standard constituent quark model to describe the basic properties of this resonance, such as its mass and photocouplings, and their Q^2 evolution. Quark models utilizing a harmonic or linear confining potential predict a normal level ordering of radial and orbital nucleon excitations according to parity, which is violated by the unusually low Roper mass. This has raised questions about the mechanism for breaking SU(6) symmetry in resonances, and alternatives to non-relativistic models with color-spin interactions [2] between massive quarks have appeared. These include

relativistic treatments [3], such as modeling the Roper on the light-cone [4], or as a hybrid baryon ($q^3 g$) where the state is assumed to have a large gluonic component [5], or as a baryon with a small quark core and a large meson cloud [6], or as a $N\sigma$ molecule [7], or even as a member of the pentaquark octet [8]. Finally, recent quenched lattice QCD calculations [9] have shown that the observed level ordering of the Roper emerges only in the chiral limit of vanishing quark mass.

The large variety of quark models make very distinct predictions for the internal structure of the Roper, which can be tested by measuring the Q^2 dependence of the transverse $A_{1/2}^p$ and scalar $S_{1/2}^p$ photocoupling amplitudes. For example, the three-quark (q^3) state is predicted to have a characteristically slow falloff of $A_{1/2}^p$ and $S_{1/2}^p$. On the other hand, for the hybrid ($q^3 g$) state $A_{1/2}^p(Q^2)$ is predicted to be more similar to the rapid falloff of the $N \rightarrow \Delta(1232)$ transition, while $S_{1/2}^p(Q^2) = 0$. Accurate knowledge of the Roper transition form factors therefore has significant implications for models of nucleon structure and understanding of the confinement mechanism.

Electromagnetic studies of the Roper resonance have up to now been limited by the Roper's large width (≈ 350 MeV) [10] and small photoproduction cross section. Additionally, many of the data used for such studies involve the $\pi^0 p$ final state, although the $\pi^+ n$ channel is more favorable due to the larger sensitivity to $I=1/2$ states. Par-

*Current address:University of New Hampshire, Durham, New Hampshire 03824-3568

†Current address:Sakarya University, Sakarya, Turkey

‡Current address:Systems Planning and Analysis, Alexandria, Virginia 22311

§Current address:Catholic University of America, Washington, D.C. 20064

¶Current address:University of South Carolina, Columbia, South Carolina 29208

**Current address:Massachusetts Institute of Technology, Cambridge, Massachusetts 02139-4307

††Current address:Physikalisches Institut der Universitaet Giessen, 35392 Giessen, Germany

‡‡Current address:University of Massachusetts, Amherst, Massachusetts 01003

tial wave analysis (PWA) fits of cross-section measurements are necessary to separate the weak Roper excitation multipoles from non-resonant backgrounds and the tails of adjacent resonances. However the reliability of this separation cannot be verified except through analysis of additional experimental observables. In particular, the polarized structure function $\sigma_{LT'}$ in pion electroproduction measures the imaginary part of the interference between longitudinal (L) and transverse (T) amplitudes:

$$\text{Im}(L^*T) = \text{Re}(L)\text{Im}(T) - \text{Im}(L)\text{Re}(T) \quad (1)$$

which can provide a powerful constraint to PWA fits.

Recent measurements of $\sigma_{LT'}$ in the $\Delta(1232)$ region [11, 12] showed a strong interference between the dominant M_{1+} resonant multipole and largely real non-resonant backgrounds, as shown schematically in Figure 1 (left). In particular, the $\sigma_{LT'}(\pi^+n)$ channel [12] was well described by several phenomenological unitary models, indicating that the dominant t -channel pion pole and Born terms are under control. These Born contributions also determine the real parts of non-resonant multipoles in the Roper resonance region and under the conditions illustrated in Figure 1 (right) can greatly amplify the small imaginary Roper resonant multipoles.

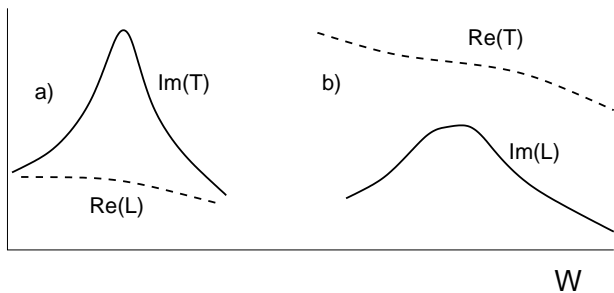


FIG. 1: Illustration of how $\text{Im}(L^*T)$ term can reveal different physics backgrounds. a) Weak background $\text{Re}(L)$ buried under strong resonance $\text{Im}(T)$. b) Weak resonance $\text{Im}(L)$ buried under strong background $\text{Re}(T)$. In each case interference through Eq. 1 allows the stronger amplitude to amplify the weaker amplitude, making the latter experimentally accessible.

In this Brief Report we present the first measurements of $\sigma_{LT'}$ obtained in the Roper resonance region using the $p(\vec{e}, e'p^+)n$ and $p(\vec{e}, e'p)\pi^0$ reactions. The data reported here span the invariant mass interval $W = 1.1 - 1.6$ GeV at $Q^2 = 0.40$ and 0.65 GeV², and cover the full angular range in the πN center-of-mass (c.m.). These data were taken simultaneously with previous measurements in the $\Delta(1232)$ region reported earlier [11, 12].

The experiment was performed at the Thomas Jefferson National Accelerator Facility (Jefferson Lab) using a 1.515 GeV, 100% duty-cycle beam of longitudinally polarized electrons incident on a liquid-hydrogen target. The electron polarization was determined by Møller polarimeter measurements to be $0.690 \pm$

$0.009(\text{stat.}) \pm 0.013(\text{syst.})$. Scattered electrons and pions were detected in the CLAS spectrometer [13]. Electron triggers were enabled through a hardware coincidence of the gas Čerenkov counters and the lead-scintillator electromagnetic calorimeters. Particle identification was accomplished using momentum reconstruction in the tracking system and time-of-flight from the target to the scintillators. Software fiducial cuts were used to exclude regions of non-uniform detector response. Kinematic corrections were applied to compensate for drift chamber misalignments and uncertainties in the magnetic field. The πN final state was identified using cuts on the missing hadronic mass. Target window backgrounds were suppressed with cuts on the reconstructed vertex.

The single pion electroproduction cross section is given by:

$$\frac{d^4\sigma^h}{dQ^2 dW d\Omega_\pi^*} = J \Gamma_v \frac{d^2\sigma^h}{d\Omega_\pi^*}, \quad (2)$$

where Γ_v is the virtual photon flux and the Jacobian $J = \partial(E', \cos \theta_e) / \partial(Q^2, W)$ relates the differential volume element $dQ^2 dW$ of the binned data to the measured electron kinematics $dE' d\cos \theta_e$. Here $d^2\sigma^h$ is the c.m. differential cross section for $\gamma^* p \rightarrow \pi N$ with the electron beam helicity h . For an unpolarized target $d^2\sigma^h$ depends on the transverse ϵ and longitudinal ϵ_L polarization of the virtual photon through five structure functions: $\sigma_T, \sigma_L, \sigma_{TT}$, and the transverse-longitudinal interference terms σ_{LT} and $\sigma_{LT'}$:

$$\begin{aligned} \frac{d^2\sigma^h}{d\Omega_\pi^*} &= \frac{p_\pi^*}{k_\gamma^*} (\sigma_0 + h \sqrt{2\epsilon_L(1-\epsilon)} \sigma_{LT'} \sin \theta_\pi^* \sin \phi_\pi^*), \\ \sigma_0 &= \sigma_T + \epsilon_L \sigma_L + \epsilon \sigma_{TT} \sin^2 \theta_\pi^* \cos 2\phi_\pi^* \\ &\quad + \sqrt{2\epsilon_L(1+\epsilon)} \sigma_{LT} \sin \theta_\pi^* \cos \phi_\pi^*, \end{aligned} \quad (3)$$

where p_π^* and θ_π^* are the πN c.m. momentum and polar angle, ϕ_π^* is the azimuthal rotation of the hadronic plane with respect to the electron scattering plane, $\epsilon = (1 + 2|\vec{q}|^2 \tan^2(\theta_e/2) / Q^2)^{-1}$, $\epsilon_L = (Q^2 / |k^*|^2) \epsilon$, $|k^*|$ is the virtual photon c.m. momentum, and k_γ^* is the real photon equivalent energy.

Determination of $\sigma_{LT'}$ was made through the beam spin asymmetry $A_{LT'}$:

$$A_{LT'} = \frac{d^2\sigma^+ - d^2\sigma^-}{d^2\sigma^+ + d^2\sigma^-} \quad (4)$$

$$= \frac{\sqrt{2\epsilon_L(1-\epsilon)} \sigma_{LT'} \sin \theta_\pi^* \sin \phi_\pi^*}{\sigma_0}. \quad (5)$$

The value of $A_{LT'}$ was obtained for individual bins of $(Q^2, W, \cos \theta_\pi^*, \phi_\pi^*)$ by dividing the measured asymmetry A_m by the magnitude of the electron beam polarization P_e :

$$A_{LT'} = \frac{A_m}{P_e} \quad (6)$$

$$A_m = \frac{N_{\pi^+} - N_{\pi^-}}{N_{\pi^+} + N_{\pi^-}}, \quad (7)$$

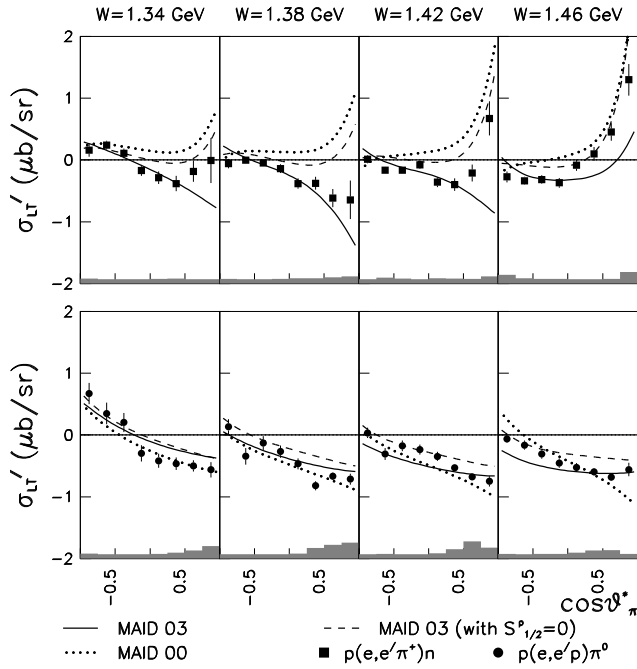


FIG. 2: CLAS measurements of $\sigma_{LT'}$ versus $\cos\theta_\pi^*$ for the π^+n channel (top) and the π^0p channel (bottom) at $Q^2=0.40$ GeV 2 and $W = 1.34 - 1.46$ GeV. The curves show model predictions discussed in the text. The shaded bars show estimated systematic errors.

where N_π^\pm is the number of livetime-corrected πN events detected for each electron beam helicity state, normalized to beam charge. Radiative corrections were applied using the program recently developed by Afanasev *et al.* for exclusive pion electroproduction [14]. Corrections were also applied to compensate for cross section variations over the width of each bin, using the MAID00 model described below. Bin full-widths were $\Delta Q^2 = 0.15$ GeV 2 , $\Delta W = 0.4$ GeV, $\Delta \cos\theta_\pi^* = 0.25$ and $\Delta\phi_\pi^* = 45^\circ$. Monte Carlo studies showed no significant helicity dependence to the CLAS acceptance, therefore no acceptance corrections to A_m were applied. Next the $A_{LT'}$ distributions were multiplied by the unpolarized cross section σ_0 , using a parameterization of measurements of σ_0 made during the same experiments [15, 16]. The structure function $\sigma_{LT'}$ was then extracted using Eq. 5 by fitting the ϕ_π^* distributions corresponding to each $\cos\theta_\pi^*$ bin. Systematic errors for $\sigma_{LT'}$ were dominated by uncertainties in the determination of the electron beam polarization and the parameterization of σ_0 . The systematic errors arising from the other corrections to A_m were negligible in comparison. Quadratic addition of the individual contributions yields a total relative systematic error of $< 6\%$ for all of our measured data points.

Figure 2 shows c.m. angular distributions of $\sigma_{LT'}$ for different W bins in the Roper resonance region at $Q^2 = 0.40$ GeV 2 . Our measurements for the π^+n channel (top) and the π^0p channel (bottom) are shown compared to the unitary isobar model of Drechsel *et al.* (MAID00

and MAID03) [17, 18], a phenomenological parameterization of previous pion photo- and electroproduction data. MAID includes all well-established resonances parameterized using Breit-Wigner functions and with backgrounds calculated from Born diagrams and t -channel vector-meson exchange. The model is unitarized according to the K -matrix approach by incorporating the πN scattering phase shifts [19] into the background amplitudes and treating the rescattered pion as on-shell. The MAID03 solution [18] was fitted to recent π^0 electroproduction cross section data from Mainz, Bates, Bonn, and JLAB, while MAID00 estimated the transverse (M_{1-}) and longitudinal (S_{1-}) Roper resonance photocouplings using older electroproduction data from the 1970s.

The structure function $\sigma_{LT'}$ determines the imaginary part of bilinear products between longitudinal and transverse amplitudes and can be expressed by the expansion:

$$\sigma_{LT'} = A + BP_1(\cos\theta_\pi^*) + CP_2(\cos\theta_\pi^*), \quad (8)$$

with

$$A = -Im(S_{0+}(M_{1-} - M_{1+} + 3E_{1+})^* + E_{0+}^*(S_{1-} - 2S_{1+}) + \dots) \quad (9)$$

$$B = -6Im(S_{1+}(M_{1-} - M_{1+} + 3E_{1+})^* + E_{1+}^*(S_{1-} - 2S_{1+}) + \dots) \quad (10)$$

$$C = -12Im((M_{2-} - E_{2-})^*S_{1+} + 2E_{1+}^*S_{2-} + \dots), \quad (11)$$

where $P_l(\cos\theta_\pi^*)$ is the l^{th} -order Legendre polynomial. Sensitivity to the Roper multipoles M_{1-}, S_{1-} occurs mainly in the A and B Legendre coefficients, through interference with the electric and Coulomb dipole and quadrupole terms. The t -channel pion pole makes substantial contributions to S_{0+}, E_{1+} and S_{1+} throughout the $\Delta(1232)$ and Roper regions, while the s -channel electric Born term saturates the E_{0+} multipole. For the π^+ channel, these multipoles are largely real and significantly larger than for the π^0 channel. As a result significant interference with the imaginary (resonant) parts of M_{1-}, S_{1-} is possible in the $\sigma_{LT'}(\pi^+n)$ observable. This is demonstrated in Figure 2, where inclusion of a non-zero longitudinal coupling $S_{1/2}^p$ for the Roper drastically changes the shape of the MAID03 predicted $\sigma_{LT'}(\pi^+n)$ angular distributions (top), while the effect on $\sigma_{LT'}(\pi^0p)$ (bottom) is much smaller.

Our previous measurements [11, 12] in the $\Delta(1232)$ resonance region were generally consistent with MAID03 for both $\sigma_{LT'}(\pi^0p)$ and $\sigma_{LT'}(\pi^+n)$. A pronounced forward peak was observed for $\sigma_{LT'}(\pi^+n)$, which arose partly from the $Im(M_{1+}^*S_{1+})$ term, but also received contributions from the interference of the $\Delta(1232)$ with the *real* parts of M_{1-}, S_{1-} . The present CLAS measurement of $\sigma_{LT'}(\pi^+n)$ in Figure 2 clearly shows a suppression of forward peaking similar to the MAID03 curve, which in this W region is due to a strong $Im(E_{1+}^*S_{1-})$ interference coming from the *imaginary* part of the S_{1-} Roper multipole in the B Legendre coefficient.

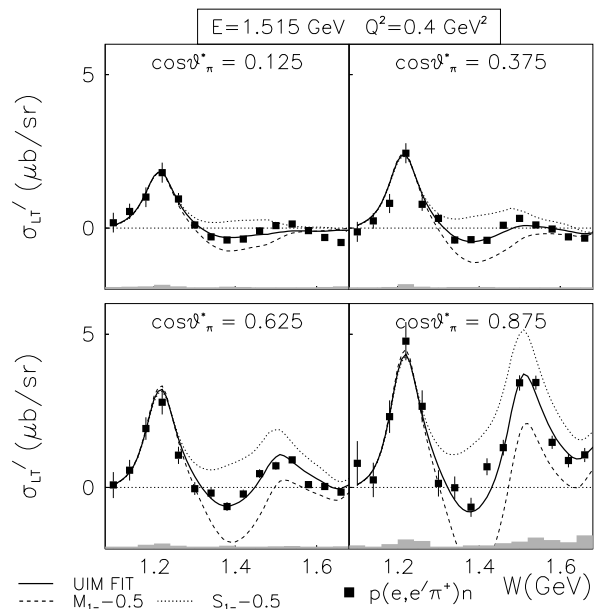


FIG. 3: CLAS measurements of $\sigma_{LT'}$ versus W (GeV) for the π^+n channel extracted at $Q^2=0.40$ GeV 2 for different $\cos\theta_\pi^*$ points. The solid line shows the best fit using the Unitary Isobar Model of Aznauryan [20]. The sensitivity of $\sigma_{LT'}$ to the Roper resonance is demonstrated by the dashed and dotted curves where the Roper contributions to M_{1-} and S_{1-} are shifted by $-0.5 \mu b^{1/2}$. The shaded bars show estimated systematic errors.

The significance of this interference is illustrated in Figure 3, which shows the W dependence of $\sigma_{LT'}(\pi^+n)$ at $Q^2 = 0.4$ GeV 2 for different $\cos\theta_\pi^*$ bins, compared with the unitary isobar model (UIM) of Aznauryan [20, 21]. The resonant photocoupling amplitudes in this model, which uses the same unitarization procedure as MAID, were determined from a global partial wave fit to all CLAS π^0 and π^+ electroproduction data (polarized and unpolarized) at $Q^2 = 0.4$ and 0.65 GeV 2 , including the data presented here. The optimal fit reported in [20] re-

quired a large longitudinal photocoupling for the Roper, and a transverse coupling near zero. Figure 3 shows the UIM fit from [20] after shifting the resonant part of each Roper multipole M_{1-} and S_{1-} by $-0.5 \mu b^{1/2}$, leaving the other at the fitted value. This shift was comparable to the final fitted value of S_{1-} . It clearly shows that the sensitivity is larger in the W region where the imaginary part of the Roper multipoles is nonzero, and maximized in the forward direction due to the interference through the pion pole term.

In summary, we report new experimental measurements of the polarized structure function $\sigma_{LT'}$ which show a large sensitivity to the Roper amplitudes in the π^+n channel through their interference with non-resonant backgrounds. This is due to a combined effect of the isospin enhancement of the π^+n channel for $I = 1/2$ resonances and the dominance of the t -channel pion pole term in the multipoles which interferes with the imaginary part of the Roper multipoles M_{1-} and S_{1-} . These data, in combination with other imaginary responses such as those extracted from recoil polarization experiments [22], will permit the most reliable determination of the resonant Roper photocoupling amplitudes. This information can hopefully inspire new calculations of the Roper transition form factor using modern hadronic models and lattice QCD.

We acknowledge the efforts of the staff of the Accelerator and Physics Divisions at the Thomas Jefferson National Accelerator Facility in their support of this experiment. This work was supported in part by the U.S. Department of Energy and National Science Foundation, an Emmy Noether Grant from the Deutsche Forschungsgemeinschaft, the French Commissariat à l'Énergie Atomique, the Italian Istituto Nazionale di Fisica Nucleare, and the Korea Research Foundation. The Southeastern Universities Research Association (SURA) operates the Thomas Jefferson National Accelerator Facility for the United States Department of Energy under contract DE-AC05-84ER40150.

-
- [1] L. Roper, Phys. Rev. **12**, 340 (1964).
[2] N. Isgur and G. Karl, Phys. Lett. B **72**, 109 (1977).
[3] S. Capstick and N. Isgur, Phys. Rev. D **34**, 2809 (1986).
[4] S. Capstick and B. D. Keister, Phys. Rev. D **51**, 3598 (1995).
[5] Z. Li and V. D. Burkert, Phys. Rev. D **46**, 70 (1992).
[6] F. Cano and P. Gonzales, Phys. Lett. B **431**, 270 (1998).
[7] O. Krehl, C. Hanhart, C. Krewald, and J. Speth, Phys. Rev. C **62**, 025207 (2000).
[8] R. Jaffe and F. Wilczek, Phys. Rev. Lett. **91**, 232003 (2003).
[9] N. Mathur et al., Phys. Lett. B **605**, 137 (2005).
[10] S. Eidelman et al., Phys. Lett. B **592**, 1 (2004).
[11] K. Joo et al., Phys. Rev. C **68**, 032201 (2003).
[12] K. Joo et al., Phys. Rev. C **70**, 042201 (2004).
[13] B. Mecking et al., Nucl. Inst. Meth. **A503**, 513 (2003).
[14] A. Afanasev, I. Akushevich, V. Burkert, and K. Joo, Phys. Rev. D **66**, 074004 (2002).
[15] H. Egiyan, Ph.D. thesis, William and Mary (2001).
[16] K. Joo et al., Phys. Rev. Lett. **88**, 122001 (2002).
[17] D. Drechsel et al., Nucl. Phys. **A645**, 145 (1999), URL www.kph.uni-mainz.de/MAID/.
[18] L. Tiator et al., Eur. Phys. J **A19**, 55 (2004).
[19] R. A. Arndt, W. J. Briscoe, I. I. Strakovsky, R. L. Workman, and M. M. Pavan, Phys. Rev. C **69**, 035213 (2004).
[20] I. G. Aznauryan et al., Phys. Rev. C **71**, 015201 (2005).
[21] I. G. Aznauryan, Phys. Rev. C **67**, 015209 (2003).
[22] J. J. Kelly et al., nucl-ex/0509004.